Thermodynamic properties of the extended Hubbard model with strong intra-atomic attraction and an arbitrary electron density

S. Robaszkiewicz
Institute of Physics, A. Mickiewicz University, Poznán, Poland

R. Micnas
Institute de Physics, A. Mickiewicz Univeristy, Poznán, Poland, and Departamento de Engenharia Espacial, Instituto de Pesquisas Espaciais, Conselho Nacional de Desenvolvimento Científico e Tecnológico, 12200, S. J. dos Campos, SP, Brazil*

K. A. Chao
Department of Physics and Measurement Technology, University of Linköping, Linköping, Sweden
(Received 24 April 1980)

We have used a canonical transformation to derive an effective extended Hubbard Hamiltonian with intra-atomic repulsion and Ising-type interatomic exchange interaction in an effective external magnetic field from the extended Hubbard model with intra-atomic attraction. The absence of magnetic ordering in the original Hamiltonian is transformed into the condition of one quasiparticle per atom. In the strong–intra-atomic–attraction limit, we can further derive from the transformed Hamiltonian an antiferromagnetic anisotropic Heisenberg Hamiltonian in an external field and with a given value of magnetization. A phase diagram of the charge-ordered, the singlet-superconducting, the mixed, and the nonordered phase is then obtained with the mean-field approximation. We continue to investigate the collective excitations in the MFA states. For various special cases our results reduce to the known results or the exact solutions.

I. INTRODUCTION

Much of the investigations of low-dimensional systems are devoted to the understanding of their low-temperature behaviors in terms of various phase transitions which are related to the metal-nonmetal transition phenomena and the possibility of having high-temperature superconductivity. The central theme of such investigations is the role of the effective intra-atomic electron attraction which can be derived from the coupling between electrons and intramolecular vibrations or electronic excited states,[1–4] or between electrons in different bands in a chemical complex.[5] Two models have been considered extensively: an extension of the Luttinger or Tomonaga model has been studied by many authors[6–14] and a modified Hubbard model by the others.[2–4,15–25] While the former is mostly restricted to the quasi-one-dimensional systems, the latter can be easily generalized to the case of three dimensions.

The Hubbard model with attractive intra-atomic interaction (AII), i.e., with $U < 0$ has been used by Anderson,[26] Street and Mott,[27] and Adler and Yoffa[28] to interpret the electrical, magnetic, and optical properties of amorphous materials. The work has been extended by Chakraverty *et al.*[29] using a two-site Hubbard model. Ionova *et al.*[5] and Lubimov *et al.*[30] suggest the use of such a model with AII to explain the alternating-valence ordering observed in some inorganic compounds with mixed valences.[31,32] For the half-filled Hubbard model with AII, mean-field approximation[33,34] and the solution derived from the functional-integral method[35,36] as well as from the variational treatment[37] predict charge-ordered solutions in the large $|U|$ limit. On the other hand, Brouers[38] has shown the absence of charge ordering in the framework of the Hubbard III Green's-function decoupling scheme.

Very few exact results exist for the Hubbard model with AII. For the one-dimensional case the exact ground-state energy has been determined by Shiba[16] for one electron per atom $n = 1$, and by Krivnov and Ovchinnikov[39] for arbitrary electron density. It has also been predicted[15–17] that for $n = 1$ the magnetic susceptibility is strongly suppressed by the AII as compared to the case of $U > 0$, and that it tends to zero as $T \to 0$. Moreover, Krivnov and Ovchinnikov[39] have shown that the single-particle excitation spectrum has a gap for arbitrary electron density, contrary to the case of $U > 0$, where such gap exists only for $n = 1$.[40]

Recently an extended Hubbard model (for both $U > 0$ and $U < 0$) including the interatomic electron interactions has also been analyzed for the case of weakly coupled one-dimensional chains.[19–21,23] In the limit of strong AII it has been shown by elementary

degenerate perturbation theory that the model is equivalent to a weakly interacting array of anisotropic Heisenberg spin chains. Therefore, for the case of half-filled band the electronic correlation functions for the extended Hubbard model can be derived from the known corresponding ones of the pseudospin system. Based on this equivalence, one obtains the phase transitions leading to the singlet superconducting state and the charge-density wave in coupled chains.

The purpose of the present work is to investigate the extended Hubbard model with AII and arbitrary electron density. In Sec. II we will perform a canonical transformation to derive an equivalent model Hamiltonian with $U>0$ from the extended Hubbard Hamiltonian with $U<0$. This allows us to study the physical properties of the latter on the basis of the known results of the former. The rest is devoted to the limit of strong AII for which the model Hamiltonian reduces further to an effective pseudospin Hamiltonian. We then obtain the phase diagram within the framework of the mean-field approximation (MFA) for arbitrary electron density in Sec. III. The collective excitation will be studied in Sec. IV, followed by a concluding remark in Sec. V.

II. CANONICAL TRANSFORMATION AND EFFECTIVE PESUDOSPIN HAMILTONIAN

We start from the extended Hubbard model with intra-atomic attraction

$$H=\sum_{ij\sigma}{}' t_{ij}c_{i\sigma}^{\dagger}c_{j\sigma}-\frac{1}{2}|U|\sum_{i\sigma}n_{i\sigma}n_{i-\sigma}+\frac{1}{2}\sum_{ij\sigma\sigma'}{}' W_{ij}n_{i\sigma}n_{j\sigma'}+\sum_{i\sigma}(E_i-\mu)n_{i\sigma} \quad , \tag{2.1}$$

where $c_{i\sigma}^{\dagger}$, $c_{i\sigma}$, and $n_{i\sigma}$ are, respectively, the creation, the destruction, and the number operators associated to the localized orbital at site i. t_{ij} is the hopping integral and $-|U|$ is the intra-atomic attraction energy. The interatomic interaction energy W_{ij} is assumed in this paper to be spin independent for simplicity. The single-site energy E_i may be site dependent, and μ is the chemical potential. The primed sum in Eq. (2.1) excludes terms with $i=j$.

We consider a system consisting of N_e electrons and N atoms. The electron density

$$n=N_e/N=\sum_{i\sigma}\langle n_{i\sigma}\rangle/N \tag{2.2}$$

has the value between 0 and 2. The first term in the Hamiltonian Eq. (2.1) is of the Bloch-electron character and so will not yield any magnetic ordering. No magnetic ordering can be introduced by the third and the fourth terms in H since they are spin independent. The second term in Eq. (2.1) favors the formation of pairs of antiparallel spin electrons on the various sites. Therefore, the ground state of H exhibits no magneitc ordering. In this paper, we will restrict ourselves to the case where the two penetrating sublattices can be defined. Consequently, we will write down the conditions that the ground state can neither be ferromagnetic nor antiferromagnetic

$$\sum_i\frac{\langle\sigma_i^{\alpha}\rangle}{N}=0 \quad , \qquad \sum_i\exp(i\vec{Q}\cdot\vec{R}_i)\frac{\langle\sigma_i^{\alpha}\rangle}{N}=0 \quad , \tag{2.3}$$

where σ_i^{α} is the $\alpha=+,-,z$ component of the spin operator $\vec{\sigma}_i$ for an electron at the lattice site $\vec{R}_i$. $\vec{Q}$ satisfies the condition $\exp(i\vec{Q}\cdot\vec{R})=-1$ for any translation $\vec{R}$ which transforms one sublattice into the other. For such systems with sublattices, the band energies satisfy the perfect nesting condition

$$\epsilon(\vec{\lambda}+\vec{Q})=-\epsilon(\vec{\lambda}) \quad , \tag{2.4}$$

where

$$\epsilon(\vec{\lambda})=\frac{1}{N}\sum_{i-j}\exp[i\vec{\lambda}\,(\vec{R}_i-\vec{R}_j)]t_{ij} \quad .$$

A. Canonical transformation

Let us perform the canonical transformation[16,18,41,42]

$$c_{i\downarrow}^{\dagger}=\exp(i\vec{Q}\cdot\vec{R}_i)b_{i\downarrow}, \quad c_{i\uparrow}^{\dagger}=b_{i\uparrow}^{\dagger} \quad , \qquad c_{i\downarrow}=\exp(-i\vec{Q}\cdot\vec{R}_i)b_{i\downarrow}^{\dagger}, \quad c_{i\uparrow}=b_{i\uparrow} \quad . \tag{2.5}$$

Then the spin operators σ_i^{α} are transformed to

$$\sigma_i^{+}=(\sigma_i^{-})^{\dagger}=c_{i\uparrow}^{\dagger}c_{i\downarrow}=\exp(-i\vec{Q}\cdot\vec{R}_i)\bar{\rho}_i^{+} \quad , \tag{2.6a}$$

$$\sigma_i^{z}=\tfrac{1}{2}(n_{i\uparrow}-n_{i\downarrow})=\bar{\rho}_i^{z} \quad , \tag{2.6b}$$

where

$$\bar{\rho}_i^{+}=(\bar{\rho}_i^{-})^{\dagger}=b_{i\uparrow}^{\dagger}b_{i\downarrow}^{\dagger} \quad , \tag{2.6c}$$

$$\bar{\rho}_i^{z}=\tfrac{1}{2}(\bar{n}_{i\uparrow}+\bar{n}_{i\downarrow}-1) \quad , \tag{2.6d}$$

$$\bar{n}_{i\sigma}=b_{i\sigma}^{\dagger}b_{i\sigma} \quad . \tag{2.6e}$$

On the other hand, the charge operators are transformed to

$$\rho_i^{+}=(\rho_i^{-})^{\dagger}=c_{i\uparrow}^{\dagger}c_{i\downarrow}^{\dagger}=\exp(i\vec{Q}\cdot\vec{R}_i)\bar{\sigma}_i^{+} \quad , \tag{2.7a}$$

$$\rho_i^{z}=\tfrac{1}{2}(n_{i\uparrow}+n_{i\downarrow}-1)=\bar{\sigma}_i^{z} \quad , \tag{2.7b}$$

where

$$\bar{\sigma}_i^{+}=b_{i\uparrow}^{\dagger}b_{i\downarrow} \quad , \tag{2.7c}$$

$$\bar{\sigma}_i^{z}=\tfrac{1}{2}(\bar{n}_{i\uparrow}-\bar{n}_{i\downarrow}) \quad . \tag{2.7d}$$

Therefore, within a phase factor $\exp(\pm i\vec{Q}\cdot\vec{R}_i)$ the charge operators $\bar{\rho}_i^{\alpha}$ in the new representation (the $\{b_{i\sigma}, b_{i\sigma}^{\dagger}\}$ representation) play the roles of the spin operators σ_i^{α} in the old representation (the $\{c_{i\sigma}, c_{i\sigma}^{\dagger}\}$ representation), and vice versa. It is easy to see that the operators ρ_i^{α}, $\bar{\sigma}_i^{\alpha}$, and $\bar{\rho}_i^{\alpha}$ all obey the same commutation rules as the spin operators σ_i^{α}.

The canonically transformed Hamiltonian of Eq. (2.1) has the form

$$H = \sum_{ij\sigma}{}' t_{ij} b_{i\sigma}^{\dagger} b_{j\sigma} + \tfrac{1}{2}|U| \sum_{i\sigma} \bar{n}_{i\sigma}\bar{n}_{i-\sigma} + 2\sum_{ij} W_{ij}\bar{\sigma}_i^z\bar{\sigma}_j^z + 2\sum_i (E_i-\bar{\mu})\bar{\sigma}_i^z - \tfrac{1}{2}|U| \sum_{i\sigma}\bar{n}_{i\sigma} - (\bar{\mu} - \tfrac{1}{2}|U| + \tfrac{1}{2}ZW)N \ , \quad (2.8)$$

where

$$\bar{\mu} = \mu + \tfrac{1}{2}|U| - ZW \ , \quad (2.9)$$

Z is the number of nearest neighbors, and W is the nearest-neighbor interaction energy. After the canonical transformation, Eqs. (2.2) and (2.3) provide the following auxiliary conditions:

$$\frac{2}{N}\sum_i \langle \bar{\sigma}_i^z \rangle = n - 1 \ , \quad (2.10)$$

$$\frac{1}{N}\sum_{i\sigma}\langle \bar{n}_{i\sigma}\rangle = 1 \ , \quad (2.11)$$

$$\sum_i \langle \bar{\rho}_i^{\pm}\rangle \exp(\mp i\vec{Q}\cdot\vec{R}_i) = 0 \ ,$$

$$\sum_i \bar{n}_{i\sigma}\exp(i\vec{Q}\cdot\vec{R}_i) = 0 \ , \quad (2.12)$$

$$\sum_i \langle \bar{\rho}_i^{\pm}\rangle = 0 \ .$$

Equations (2.8)–(2.12) show that the extended Hubbard Hamiltonian Eq. (2.1) of N atoms and N_e electrons with intra-atomic *attraction* and *spin-independent* interatomic W_{ij} has been transformed into an extended Hubbard Hamiltonian of *one electron per atom* with intra-atomic *repulsion* and *Ising-type interatomic exchange* interaction in the effective *external* magnetic field $(E_i - \bar{\mu})$ along the z direction. The magnetization of the transformed system along the z direction has a fixed value given by Eq. (2.10). By the same token that there is no magnetic ordering in the ground state of the original Hamiltonian Eq. (2.1), Eqs. (2.11) and (2.12) indicate that there is neither superconducting nor charge ordering in the ground state of the transformed Hamiltonian Eq. (2.8). We should point out that although the original Hamiltonian has rotational symmetry in spin space, the canonical transformation Eq. (2.5) does not preserve such symmetry except for the special case $n = 1$, $W_{ij} = 0$, and $E_i = E_0 = \bar{\mu}$.

B. Phase diagram of Hubbard model with AII

From Eqs. (2.5) to (2.7d), we readily obtain

$$\frac{1}{N}\sum_i \langle \bar{\sigma}_i^{+}\rangle \exp(i\vec{Q}\cdot\vec{R}_i) = \frac{1}{N}\sum_i \langle c_{i\uparrow}^{\dagger} c_{i\downarrow}^{\dagger}\rangle = \frac{1}{N}\sum_i \langle \rho_i^{+}\rangle \ , \quad (2.13a)$$

$$\frac{1}{N}\sum_i \langle \bar{\sigma}_i^{+}\rangle = \frac{1}{N}\sum_i \langle c_{i\uparrow}^{\dagger} c_{i\downarrow}^{\dagger}\rangle \exp(-i\vec{Q}\cdot\vec{R}_i) = \frac{1}{N}\sum_i \langle \rho_i^{+}\rangle \exp(-i\vec{Q}\cdot\vec{R}_i) \ , \quad (2.13b)$$

$$\frac{1}{N}\sum_i \langle \bar{\sigma}_i^{z}\rangle \exp(i\vec{Q}\cdot\vec{R}_i) = \frac{1}{2N}\sum_i \langle n_{i\uparrow} + n_{i\downarrow} - 1\rangle \exp(i\vec{Q}\cdot\vec{R}_i) = \frac{1}{N}\sum_i \langle \rho_i^{z}\rangle \exp(i\vec{Q}\cdot\vec{R}_i) \ . \quad (2.14)$$

The quantities at the left-hand side of the above equations measure the magnetic long-range order (LRO) in the canonically transformed Hamiltonian Eq. (2.8), while those at the right-hand side measure the singlet-superconducting or the charge LRO in the original Hamiltonian Eq. (2.1). Equations (2.13a) and (2.13b) indicate that the magnetic order in the XY plane, namely, the off-diagonal LRO (ODLRO) in the transformed Hamiltonian corresponds to the singlet-superconducting order in the original Hamiltonian. From Eq. (2.14) we see that the nonuniform magnetic order along the z axis, i.e., the diagonal LRO (DLRO) in the transformed Hamiltonian corresponds to the charge order in the original Hamiltonian. These equivalences are summarized in Table I. We should point out the remarkable similarity between the present situation and the case of liquid helium where such equivalence was derived many years ago.[43] Nevertheless, our further analysis will show that the thermodynamic properties of these two cases are different.

Based on the correspondence listed in Table I, some physical properties of the extended Hubbard Hamiltonian with AII can be obtained from the known properties of the transformed Hamiltonian Eq. (2.8). Let us first consider the case $n = 1$, $W_{ij} = 0$, and $E_i = E_0$ [then from Eq. (2.10) we have $E_0 - \bar{\mu} = 0$] for which Eq. (2.8) turns out to be the ordinary Hubbard Hamiltonian. Therefore, all the physical quantities determined by the one-particle correlation function are independent of the sign of U. It may not be so for those physical quantities determined by the two-particle correlation function. For example, the magnetic susceptibility is evidently suppressed by the attractive interaction as compared

TABLE I. Corresponding phases between the Hamiltonians Eqs. (2.1) and (2.8).

Long-range order (LRO) Diagonal LRO	Off-diagonal LRO	Magnetic order in transformed Hamiltonian Eq. (2.8)	Type of ordered state in extended Hubbard model with AII Eq. (2.1)
No	No	Ferromagnetic or paramagnetic	Nonordered phase (NO) Normal metal or phase of uncorrelated pairs
Yes	No	Antiferromagnetic or complicated nonuniform order in z axis	Charge order (CO)
No	Yes	Spin flopped	Singlet superconducting (SS)
Yes	Yes	Intermediate state	Mixed phase of CO and SS (M)

to its value for the case of intra-atomic repulsion.[15,17]

It is generally accepted for the ordinary Hubbard model that the antiferromagnetic order should occur at low temperature and at the large U limit, at least for three-dimensional lattices. However, due to the rotational symmetry the sublattice magnetization can point in any direction. Consequently, when transformed back to the Hubbard model with AII, such a symmetry property makes the singlet-superconducting (SS) and the charge-ordered (CO) states degenerate and so both kinds of the LRO can exist with arbitrary weights.[18,42] The degeneracy will be removed by the interatomic interaction W_{ij}. If $W_{ij} > 0$ the antiferromagnetic order along the z axis will be stabilized. On the other hand, if $W_{ij} < 0$, the magnetic order within the XY plane will be stabilized. So for $n = 1$, the case of $W_{ij} = 0$ is just the borderline between the regions of pure SS (for $W_{ij} < 0$) and pure CO (for $W_{ij} > 0$) phases.

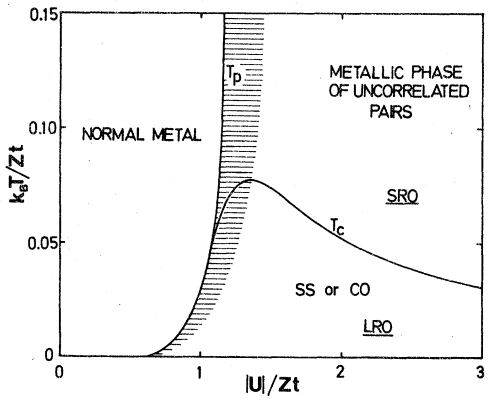

FIG. 1. Phase diagram of the half-filled Hubbard model with intra-atomic attraction. T_c and T_p denote the critical temperatures for the onset of long-range ordering and for the breaking of electronic pairs, respectively.

Recently, the phase diagram of the ordinary Hubbard model with $n = 1$ has been derived by Economou and co-workers.[44] Via the canonical transformation, this phase diagram can be mapped into the one for the Hubbard model with AII as shown in Fig. 1. In the region with LRO we expect gapless two-electron excitations from the SS state, whereas the one-electron excitations from the CO state have a gap. In the region with short-range order (SRO), the system behaves as a normal resistive metal with charge unit $2e$ but with the magnetic susceptibility strongly suppressed.

The phase diagram for the general case $n \neq 1$, $W_{ij} \neq 0$, and $E_i \neq E_0$ is very difficult to obtain. The rest of this paper will be devoted to the problem of large $|U|$ limit, while the situation of weak and intermediate coupling will be discussed in a separate paper.

C. Effective pseudospin Hamiltonian at the strong-coupling limit

Because of the condition (2.11) that there is just one quasiparticle per atom, the degenerate perturbation theory can be applied to the Hamiltonian Eq. (2.8) at the strong-coupling limit $|U| \gg t_{ij}$.[45] To the second order in $t_{ij}/|U|$ we have

$$H = \sum_{ij}{}' J_{ij}(\vec{\sigma}_i \cdot \vec{\sigma}_j - \tfrac{1}{4}) + \sum_{ij}{}' 2W_{ij}\bar{\sigma}_i^z\bar{\sigma}_j^z + 2\sum_i (E_i - \bar{\mu})(\bar{\sigma}_i^z + \tfrac{1}{2}) - \tfrac{1}{2}ZWN \ , \quad (2.15)$$

where

$$J_{ij} = 2t_{ij}^2/|U| \ . \quad (2.16)$$

Equation (2.15) had the form of an antiferromagnetic anisotropic Heisenberg Hamiltonian with a random external magnetic field. According to Eq. (2.10), the magnetization of the system along the z axis has a fixed value $\frac{1}{2}(n-1)$.

Using Eq. (2.5), we can rewrite Eq. (2.15) in terms of the $\{c_{i\sigma}, c_{i\sigma}^{\dagger}\}$ operators as

$$H=-\sum_{ij}{}' J_{ij}\rho_i^+\rho_j^- + \sum_{ij}{}' (J_{ij}+2W_{ij})\rho_i^z\rho_j^z + 2\sum_i (E_i-\bar{\mu})(\rho_i^z+\tfrac{1}{2}) - \tfrac{1}{4}N(J_0+2W_0) \quad , (2.17)$$

where $W_0=ZW$, $J_0=ZJ$, and J is the nearest neighbor J_{ij}. In terms of the same set of operators, Eq. (2.10) becomes

$$\frac{1}{N}\sum_i \langle \rho_i^z\rangle = \tfrac{1}{2}(n-1) \quad . \tag{2.18}$$

Since the operators ρ_i^{α} obey the same commutation rules as the spin operators, σ_i^{α}, ρ_i^{α} can be considered as pseudospin operators and we called Eq. (2.17) the effective pseudospin Hamiltonian. We should point out that for $E_i=0$, the pseudospin Hamiltonian is just the same as the one derived by Emery.[19]

III. PHASE DIAGRAM

With the pseudospin Hamiltonian defined for arbitrary value of the *bare electron density* n, we proceed to obtain the phase diagram for the nonrandom case $E_i=E_0$, using the MFA and the random-phase approximation (RPA). Let us change the notation to use S_i^{α} instead of ρ_i^{α}. Omitting the constant energy in Eq. (2.17), we can rewrite Eqs. (2.17) and (2.18) as

$$H=-\sum_{ij}{}' J_{ij}(S_i^xS_j^x+S_i^yS_j^y)+\sum_{ij}{}' K_{ij}S_i^zS_j^z - B\sum_i (2S_i^z+1) \quad , \tag{3.1}$$

$$\frac{1}{N}\sum_i \langle S_i^z\rangle = \tfrac{1}{2}(n-1) \quad , \tag{3.2}$$

where $K_{ij}=J_{ij}+2W_{ij}$ and the effective magnetic field B is

$$B=\bar{\mu}-E_0=\mu+\tfrac{1}{2}|U|-W_0-E_0 \quad . \tag{3.3}$$

The Hamiltonian Eq. (3.1) has been extensively studied in the theory of magnetism[46,47] as well as of liquid helium.[43,48,49] However, in our case, the effective field B is determined self-consistently through Eq. (3.2). Therefore, we are essentially dealing with an antiferromagnet in a temperature-dependent magnetic field B. Since the direction of pesudospins in the XY plane is not specified, it is sufficient to consider the possible magnetic ordering in the XZ plane.

We will formulate the MFA following the Bogoliubov variational principle.[50] If H_0 is the trial Hamiltonian, then an upper bound for the exact free energy is given by

$$F\leq F_0=-\frac{1}{\beta}\ln \mathrm{Tr}[\exp(-\beta H_0)]+\langle H-H_0\rangle_0 \quad , \tag{3.4}$$

where $\beta=1/k_BT$ and $\langle\cdots\rangle_0$ is the thermal average with respect to the trial Hamiltonian H_0. H_0 can be chosen as

$$H_0=-\sum_i \vec{\Lambda}_i\cdot\vec{S}_i - B\sum_i (2S_i^z+1) \quad , \tag{3.5}$$

with the molecular fields $\vec{\Lambda}_i$ as variational parameters to minimize the free energy F_0. After standard calculation, one obtains

$$\Lambda_i^x=\Lambda_i^y=2\sum_j J_{ij}\langle S_j^x\rangle_0 \quad , \tag{3.6a}$$

$$\Lambda_i^z=2\left[B-\sum_j K_{ij}\langle S_j^z\rangle_0\right] \quad . \tag{3.6b}$$

For a system with two interpenetrating sublattices labeled by $\gamma=A,B$ it is easy to show that the trial Hamiltonian H_0 of Eq. (3.5) has the eigenfunctions

$$|+\rangle_{\gamma}=\cos(\tfrac{1}{2}\theta_{\gamma})|\tfrac{1}{2}\rangle+\sin(\tfrac{1}{2}\theta_{\gamma})|-\tfrac{1}{2}\rangle \quad , \tag{3.7a}$$

$$|-\rangle_{\gamma}=-\sin(\tfrac{1}{2}\theta_{\gamma})|\tfrac{1}{2}\rangle+\cos(\tfrac{1}{2}\theta_{\gamma})|-\tfrac{1}{2}\rangle \quad , \tag{3.7b}$$

with the corresponding eigenenergies

$$E_A^{\pm}=-B\mp\Delta_B \quad , \tag{3.8a}$$

$$E_B^{\pm}=-B\mp\Delta_A \quad , \tag{3.8b}$$

$$\Delta_{\gamma}^2=(B-K_0\langle S_{\gamma}^z\rangle_0)^2+J_0^2\langle S_{\gamma}^x\rangle_0^2 \quad , \tag{3.9}$$

where $|\frac{1}{2}\rangle$ and $|-\frac{1}{2}\rangle$ are the two spin eigenstates, and $K_0=J_0+2W_0$. $\langle S_{\gamma}^x\rangle_0$ and $\langle S_{\gamma}^z\rangle_0$ satisfy the equations

$$\langle S_{\gamma}^x\rangle_0=(J_0\langle S_{\gamma'}^x\rangle_0/2\Delta_{\gamma'})\tanh\beta\Delta_{\gamma'} \quad , \tag{3.10a}$$

$$\langle S_{\gamma}^z\rangle_0=[(B-K_0\langle S_{\gamma'}^z\rangle_0)/2\Delta_{\gamma'}]\tanh\beta\Delta_{\gamma'} \quad . \tag{3.10b}$$

In the above expression we have $\gamma\neq\gamma'$. Equations (3.10a) and (3.10b) should be solved self-consistently together with Eq. (3.2) which can be rewritten as

$$\langle S_A^z\rangle_0+\langle S_B^z\rangle_0=n-1 \quad . \tag{3.11}$$

θ_A and θ_B are the angles between the magnetization and its z component in sublattices A and B, respectively. From Eqs. (3.10a) and (3.10b), we have

$$\tan\theta_A=\langle S_A^x\rangle_0/\langle S_A^z\rangle_0 = J_0\langle S_B^x\rangle_0/(B-K_0\langle S_B^z\rangle_0) \quad , \tag{3.12a}$$

$$\tan\theta_B=\langle S_B^x\rangle_0/\langle S_B^z\rangle_0 = J_0\langle S_A^x\rangle_0/(B-K_0\langle S_A^z\rangle_0) \quad . \tag{3.12b}$$

In terms of the eigensolutions, the free energy per lattice site is derived as

$$\frac{F_0}{N} = -\frac{1}{2\beta}\ln[2e^{\beta B}\cosh(\beta\Delta_A)] - \frac{1}{2\beta}\ln[2e^{\beta B}\cosh(\beta\Delta_B)] + J_0\langle S_A^x\rangle_0\langle S_B^x\rangle_0 - K_0\langle S_A^z\rangle_0\langle S_B^z\rangle_0 \quad . \quad (3.13)$$

Using Eqs. (3.12a) and (3.12b), we can rewrite the free energy as a function of θ_A and θ_B, and minimize it with respect to θ_A and θ_B. Before going further, we can draw the following conclusions from Table I: (1) $(\theta_A,\theta_B)=(0,\pi)$ and $(\theta_A,\theta_B)=(\pi,0)$ are solutions for the CO phase. (2) $\theta_A=\theta_B=0$ and $\theta_A=\theta_B=\pi$ are solutions for the NO phase. (3) The line $\theta_A=\theta_B$ excluding the points $\theta_A=\theta_B=0$ and $\theta_A=\theta_B=\pi$ is the solution for the SS phase. (4) The rest of the $\theta_A\theta_B$ plane is the solution of the M phase.

A. Ground-state phase diagram

To simplify the presentation of the phase diagram, from now on we will retain only the nearest-neighbor interaction in W_{ij} or J_{ij}. Taking the limit $\beta\to\infty$ in Eqs. (3.10a)–(3.13), one obtains

$$E_g = \langle H\rangle_0/J_0N = -\tfrac{1}{4}\sin\theta_A\sin\theta_B + (K_0/4J_0)\cos\theta_A\cos\theta_B - (B/2J_0)(\cos\theta_A+\cos\theta_B+2) \quad , \quad (3.14)$$

$$\langle S_\gamma^x\rangle_0 = \tfrac{1}{2}\sin\theta_\gamma, \quad \langle S_\gamma^z\rangle_0 = \tfrac{1}{2}\cos\theta_\gamma, \quad \gamma=A,B \quad , \quad (3.15)$$

and

$$\tfrac{1}{2}(\cos\theta_A+\cos\theta_B) = n-1 \quad . \quad (3.16)$$

The minimization of E_g with respect to θ_A and θ_B yields the conditions

$$2B\sin\theta_A = J_0\sin\theta_B\cos\theta_A + K_0\sin\theta_A\cos\theta_B \quad , \quad (3.17a)$$

$$2B\sin\theta_B = J_0\sin\theta_A\cos\theta_B + K_0\sin\theta_B\cos\theta_A \quad . \quad (3.17b)$$

If $n=1$, we have either the CO solution with $(\theta_A,\theta_B)=(0,\pi)$ or $(\theta_A,\theta_B)=(\pi,0)$, or the SS solution with $(\theta_A,\theta_B)=(\frac{1}{2}\pi,\frac{1}{2}\pi)$. By comparing the energies of the two phases, we see that the ground state is CO if $K_0>J_0$ (or $W>0$) but SS if $K_0<J_0$ (or $W<0$). For $K_0=J_0$ (or $W=0$) the CO and the SS states as well as the M state with $\theta_B=\pi-\theta_A$, $0<\theta_{A,B}<\pi$, are degenerate.

If $n\neq 1$, Eqs. (3.17a) and (3.17b) can be combined as

$$(\cos\theta_A-\cos\theta_B)(J_0+J_0\cos\theta_A\cos\theta_B - K_0\sin\theta_A\sin\theta_B) = 0 \quad . \quad (3.18)$$

Together with Eq. (3.16), we obtain two solutions.

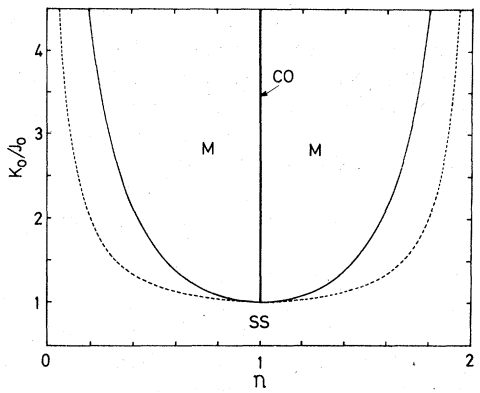

FIG. 2. Ground-state phase diagram of the Hamiltonian Eq. (2.1). The heavy vertical line is the region of charge-ordered phase. The SS-M phase boundary is given by $K_0/J_0=[1+(n-1)^2]/[1-(n-1)^2]$.

The first one is the SS solution with $\theta_A=\theta_B$, and the energy is

$$E_g(\mathrm{SS}) = -\tfrac{1}{4} - \tfrac{1}{4}(K_0/J_0+1)(n^2-1) \quad . \quad (3.19)$$

The second solution is the M solution with $\theta_A\neq\theta_B$, and the energy is

$$E_g(\mathrm{M}) = -(K_0^2/J_0^2-1)^{1/2}\tfrac{1}{2}(n-|n-1|) - K_0/4J_0 \quad . \quad (3.20)$$

By comparing $E_g(\mathrm{SS})$ and $E_g(\mathrm{M})$, the phase boundary between the SS and the M phases is determined and is shown as the solid curve in Fig. 2 together with the CO ground state indicated by the heavy vertical line.

In Fig. 3 we show the order parameters for $K_0/J_0=1.75$: curve A for $\langle S_B^x\rangle_0-\langle S_A^z\rangle_0$, curve B for

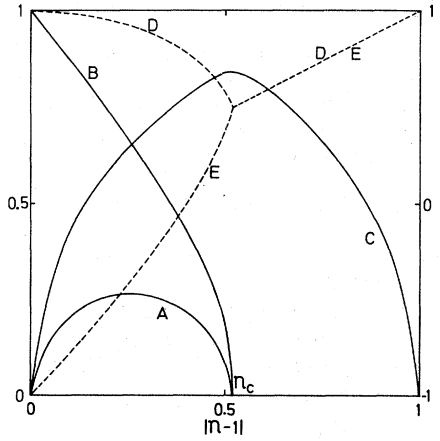

FIG. 3. Order parameters for the ground state of Eq. (2.1). Left scale is for the solid curves and the right scale is for the dashed cruves. See the text for details.

$\langle S_A^z\rangle_0 - \langle S_B^z\rangle_0$, curve C for $\langle S_A^x\rangle_0 + \langle S_B^x\rangle_0$, curve D for $\cos\theta_A$, and curve E for $\cos\theta_B$. The transition between the SS and the M phases is then of the second order. We would like to point out that in Hartree-Fock approximation the order parameter $\langle S_B^x\rangle_0 - \langle S_A^x\rangle_0$ is assumed to be zero.

B. Finite temperature phase diagram

For finite temperature, we have to solve Eqs. (3.10a)–(3.13) for all the four CO, NO, SS, and M phases to find out the stable one with minimum free energy. The mathematical manipulation is straight forward, so we will only present the final results. For the NO phase, the free energy per site is

$$F_0/N = -\frac{1}{\beta}\ln\{2e^{\beta B}\cosh\beta[B-\tfrac{1}{2}(n-1)K_0]\} - \tfrac{1}{4}(n-1)^2K_0 \ , \quad (3.21)$$

with

$$B = \frac{1}{2\beta}\ln\frac{n}{2-n} + \tfrac{1}{2}(n-1)K_0 \ . \quad (3.22)$$

If we define the order parameter $\eta = \langle S_A^z\rangle_0 - \langle S_B^z\rangle_0$, then for the CO phase we have

$$F_0/N = -\frac{1}{2\beta}\ln\{e^{\beta B}\cosh\beta[B-\tfrac{1}{2}(n-\eta-1)K_0]\} - \frac{1}{2\beta}\ln\{e^{\beta B}\cosh\beta[B-\tfrac{1}{2}(n+\eta-1)K_0]\} - \tfrac{1}{4}[(n-1)^2-\eta^2]K_0 \ , \quad (3.23)$$

with

$$\eta = \tfrac{1}{2}\tanh\beta[B-\tfrac{1}{2}(n-\eta-1)K_0] - \tfrac{1}{2}\tanh\beta[B-\tfrac{1}{2}(n+\eta-1)K_0] \ , \quad (3.24)$$

$$n-1 = \tfrac{1}{2}\tanh\beta[B-\tfrac{1}{2}(n-\eta-1)K_0] + \tfrac{1}{2}\tanh\beta[B-\tfrac{1}{2}(n+\eta-1)K_0] \ . \quad (3.25)$$

The phase transition between the NO and the CO phases is continuous and takes place at the temperature $T(\mathrm{CO})$ given by

$$T(\mathrm{CO}) = n(2-n)K_0/2k_B \ . \quad (3.26)$$

At the limit $|U|\to\infty$, $T(\mathrm{CO})$ agrees with the result obtained earlier.[22]

For the SS phase with $\theta_A = \theta_B$, we have $\langle S_A^x\rangle_0 = \langle S_B^x\rangle_0 = \langle S^x\rangle_0$ and $\langle S_A^z\rangle_0 = \langle S_B^z\rangle_0 = \langle S^z\rangle_0$. If we define $M^2 = \langle S^x\rangle_0^2 + \langle S^z\rangle_0^2$, then the free energy can be expressed as

$$F_0/N = -\frac{1}{\beta}\ln(e^{\beta B}\cosh\beta J_0 M) - J_0M^2 + (J_0+K_0)\langle S^z\rangle_0^2 \ , \quad (3.27)$$

with

$$M = \tfrac{1}{2}\tanh\beta J_0 M \quad (3.28)$$

and a temperature-independent effective field $B = (J_0+K_0)\langle S^z\rangle_0$. The continuous transition to the NO phase occurs at the temperature $T(\mathrm{SS})$ given by

$$T(\mathrm{SS}) = (n-1)J_0/k_B\ln\frac{n}{2-n} \ . \quad (3.29)$$

Finally, we will use the Landau expansion[49] to determine the boundaries between the M phase and the SS phase, and between the M phase and the CO phase. The boundary between the M and the SS phases is determined by

$$J_0[4M^2+\langle S^x\rangle_0^2(\beta J_0-4\beta J_0M^2-2)] = K_0[4M^2+(\langle S^x\rangle_0^2+2\langle S^z\rangle_0^2) \times(\beta J_0-4\beta J_0M^2-2)] \ . \quad (3.30)$$

The boundary between the M and the CO phases is obtained from solving the two coupled equations

$$\ln\{(n^2-\eta^2)/[(2-n)^2-\eta^2]\} = 2J_0[(n-1)^2+(K_0^2/J_0^2-1)\eta^2]^{1/2}/k_BT \ , \quad (3.31)$$

$$\ln[(n+\eta)(2-n+\eta)/(n-\eta)(2-n-\eta)] = 2K_0\eta/k_BT \ . \quad (3.32)$$

In Fig. 4 we show the phase diagrams for (a) $K_0/J_0=1$ (or $W=0$), (b) $K_0/J_0=1.1$ (then $W>0$),

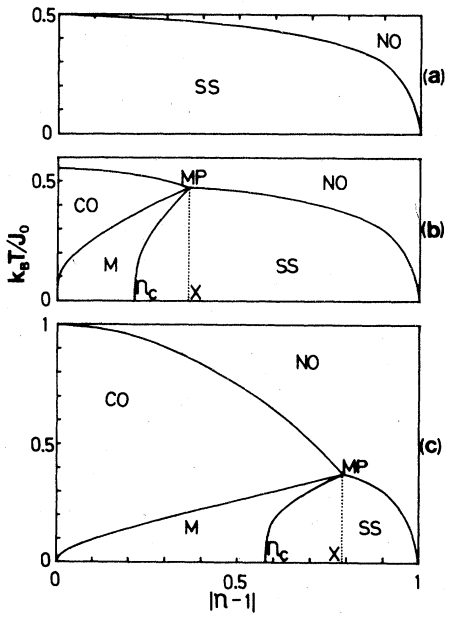

FIG. 4. Phase diagram for the Hamiltonian (2.1): (a) $K_0/J_0=1$, (b) $K_0/J_0=1.1$, and (c) $K_0/J_0=2$. See the text for details.

and (c) $K_0/J_0=2$. For $W=0$, the SS, the CO, and the M states are degenerate at $n=1$. For $W>0$ all four phases appear and the transitions among them are second order. The four critical lines meet at a multicritical point (MP) corresponding to a tetracritical point in the B-T phase diagram of an anisotropic antiferromagnet.[49,51,52] With increasing W, the MP point moves along the boundary between the SS and NO phases given by (a). This is due to the fact that in MFA the transition between the SS and NO phases is independent of W. The position X as a function of n and K_0/J_0 is shown in Fig. 2 as the dashed curve. As the temperature rises, there is only one transition SS $\rightarrow$ NO for the region below the dashed curve, but two transitions M $\rightarrow$ CO $\rightarrow$ NO for the region above the solid curve, while three transitions SS $\rightarrow$ M $\rightarrow$ CO $\rightarrow$ NO for the region between the dashed and the solid curves.

Finally, we would like to emphasize the important difference in the thermodynamic behavior between the ordinary nearest-neighbor anisotropic antiferromagnet in an external field and our pseudospin model where the effective field is induced by the canonical transformation. For the former, there are only three phases, namely, the paramagnetic (P), the antiferromagnetic (AF), and the spin-flopped (SF) phases. While the transitions AF $\leftrightarrow$ P and SF $\leftrightarrow$ P are second order, the transition AF $\leftrightarrow$ SF is first order.[51-53] For our pseudospin Hamiltonian, due to the constraint Eq. (3.11) on the magnetization, the first-order boundary for AF $\leftrightarrow$ SF splits into two second-order boundaries together with the emergence of the intermediate (M) phase and the tetracritical point.

IV. COLLECTIVE EXCITATIONS

In this section, we will investigate the elementary excitations, namely, the pseudospin waves in the MFA states. In the superconducting phase such elementary excitations represent a collective motion of the electron pairs with zero spin, or in other words, a transfer of electron pairs to a neighboring site without unpairing. On the other hand, the elementary excitations in the charge-ordered phase are of the type of electron density wave. For simplicity and yet without losing generality, in our numerical calculation we will restrict ourselves to the one-dimensional case.

We will use the Green's-function approach formulated in terms of the standard basis operators.[54,55] The standard basis operators are defined as

$$L^i_{\alpha\alpha'}=|i\alpha\rangle\langle i\alpha'| \ , \tag{4.1}$$

where i labels the position of the site and $|i\alpha\rangle$ are the states derived from the MFA given by Eqs. (3.7a) and (3.7b). The ensemble average $D^i_\alpha=\langle L^i_{\alpha\alpha}\rangle$ measures the probability that the state $|i\alpha\rangle$ is occupied and satisfies the normalization condition $\sum_{\alpha=1}^{p} D^i_\alpha=1$, where p is the number of states. Any operator A can be expressed in terms of $L^i_{\alpha\alpha'}$ as

$$A=\sum_{i\alpha\alpha'}\langle i\alpha|A|i\alpha'\rangle L^i_{\alpha\alpha'}=\sum_{i\alpha\alpha'}A^i_{\alpha\alpha'}L^i_{\alpha\alpha'} \ . \tag{4.2}$$

The pseudospin Hamiltonain Eq. (3.1) and the magnetization condition Eq. (3.2) can then be written as

$$H=-\sum_{i\alpha\alpha'}h^i_{\alpha\alpha'}L^i_{\alpha\alpha'}-\frac{1}{2}\sum_{ij\alpha\alpha'\beta\beta'}M^{ij}_{\alpha\alpha'\beta\beta'}L^i_{\alpha\alpha'}L^j_{\beta\beta'} \ , \tag{4.3}$$

$$\frac{1}{N}\sum_{i\alpha\alpha'}(S^z_i)_{\alpha\alpha'}\langle L^i_{\alpha\alpha'}\rangle=n-1 \ , \tag{4.4}$$

where

$$h^i_{\alpha\alpha'}=B[2(S^z_i)_{\alpha\alpha'}+1] \ , \tag{4.5}$$

$$M^{ij}_{\alpha\alpha'\beta\beta'}=J_{ij}[(S^+_i)_{\alpha\alpha'}(S^-_j)_{\beta\beta'}+(S^-_i)_{\alpha\alpha'}(S^+_j)_{\beta\beta'}]-2K_{ij}(S^z_i)_{\alpha\alpha'}(S^z_j)_{\beta\beta'} \ . \tag{4.6}$$

Within the RPA, the equation of motion for the double-time retarded Green's function[56]

$$G^{ij}_{\alpha\alpha'\beta\beta'}(t,t')=\langle\langle L^i_{\alpha\alpha'}(t);L^j_{\beta\beta'}(t')\rangle\rangle=-i\Theta(t-t')\langle[L^i_{\alpha\alpha'}(t),L^j_{\beta\beta'}(t')]\rangle \tag{4.7}$$

has been derived[55] as

$$(E-E^i_\alpha+E^i_{\alpha'})G^{ij}_{\alpha\alpha'\beta\beta'}(\vec{\lambda},E)+D^i_{\alpha\alpha'}\sum_{k\mu\nu}M^{ik}_{\alpha'\alpha\nu\mu}(\vec{\lambda})G^{kj}_{\nu\mu\beta\beta'}(\vec{\lambda},E)=\frac{1}{2\pi}D^i_{\alpha\alpha'}\delta_{ij}\delta_{\alpha\beta'}\delta_{\beta\alpha'} \ , \tag{4.8}$$

where $D^i_{\alpha\alpha'}=D^i_\alpha-D^i_{\alpha'}$ and

$$E^i_\alpha=h^i_{\alpha\alpha}+\sum_{\beta j}M^{ij}_{\alpha\alpha\beta\beta}(0)D^j_\beta \ . \tag{4.9}$$

The energies of the elementary excitations are temperature dependent via the occupation probability D^i_α.

In the RPA-MFA, we replace the D^i_α by its MFA value. Such approximation is equivalent to the high-density expansion method in the zeroth order.[57,58] The RPA-MFA spectrum properly reduces to the noninteracting spin-wave energy at low temperatures and provides a qualitative estimation of the temperature dependence of the spectrum in the whole range of temperatures.

In our case where two penetrating sublattices are assumed, the superscripts in Eqs. (4.7)–(4.9) can be treated as the sublattice index A and B. For the superconducting and the nonordered phases, such sublattice indices can be omitted.

A. Mixed phase

Using Eqs. (3.7a) and (3.7b) with $|i\alpha\rangle = |+\rangle_\gamma$ and $|-\rangle_\gamma$, we can easily calculate $M^{ij}_{\alpha\beta\mu\nu}(\vec{\lambda})$ and then obtain from Eq. (4.8) two equations

$$\begin{pmatrix} E-2\Delta_B & 0 & a^A_{\vec{\lambda}+} & a^A_{\vec{\lambda}-} \\ 0 & E+2\Delta_B & -a^A_{\vec{\lambda}-} & -a^A_{\vec{\lambda}+} \\ a^B_{\vec{\lambda}+} & a^B_{\vec{\lambda}-} & E-2\Delta_A & 0 \\ -a^B_{\vec{\lambda}-} & -a^B_{\vec{\lambda}+} & 0 & E+2\Delta_A \end{pmatrix} \begin{pmatrix} G^{AB}_{+-\beta\beta'}(\vec{\lambda},E) \\ G^{AB}_{-+\beta\beta'}(\vec{\lambda},E) \\ G^{BB}_{+-\beta\beta'}(\vec{\lambda},E) \\ G^{BB}_{-+\beta\beta'}(\vec{\lambda},E) \end{pmatrix} = \frac{1}{2\pi} D^B_{+-} \begin{pmatrix} 0 \\ 0 \\ \delta_{+\beta'}\delta_{\beta-} \\ -\delta_{-\beta'}\delta_{\beta+} \end{pmatrix} , \tag{4.10}$$

with $(\beta\beta') = (+-)$ and $(-+)$, respectively. In the above equation we have

$$a^i_{\vec{\lambda}\pm} = (\pm\tfrac{1}{2}J_{\vec{\lambda}} + \tfrac{1}{2}J_{\vec{\lambda}}\cos\theta_A\cos\theta_B - \tfrac{1}{2}K_{\vec{\lambda}}\sin\theta_A\sin\theta_B)D^i_{+-} , \tag{4.11}$$

where $i = A,B$ and $J_{\vec{\lambda}}$ and $K_{\vec{\lambda}}$ are, respectively, the Fourier transforms of J_{ij} and K_{ij}. Δ_A and Δ_B are given by Eq. (3.9), whereas θ_A and θ_B by Eqs. (3.12a) and (3.12b). The relationship between the occupation probability and the ensemble average of the pseudospin can be readily obtained as

$$\langle S^x_i\rangle_0 = \tfrac{1}{2}D^i_{+-}\sin\theta_i , \qquad \langle S^z_i\rangle_0 = \tfrac{1}{2}D^i_{+-}\cos\theta_i , \tag{4.12}$$

where $i = A,B$. We should remind the reader that $\langle S^z_i\rangle_0$ must satisfy the condition $\langle S^z_A\rangle_0 + \langle S^z_B\rangle_0 = n-1$, namely, Eq. (3.11).

From Eqs. (3.7a)–(3.8b) we see that at zero temperature the MFA ground state corresponds to $D^A_+ = D^B_+ = 1$ and $D^A_- = D^B_- = 0$. As shown by Eq. (3.18) that

$$J_0 + J_0\cos\theta_A\cos\theta_B - K_0\sin\theta_A\sin\theta_B = 0$$

is the solution for the mixed phase, we conclude from Eq. (4.11) that $a^A_{\vec{\lambda}+} = 0$ and $a^A_{\vec{\lambda}-} = -J_{\vec{\lambda}}$. With this information, the solutions of Eq. (4.10) are obtained as

$$E^{\pm}_{\vec{\lambda}} = \pm(\Delta_B - \Delta_A) + [(\Delta_B - \Delta_A)^2 + 4\Delta_A\Delta_B - J^2_{\vec{\lambda}}]^{1/2} , \tag{4.13}$$

where the Δ_A and Δ_B given by Eq. (3.9) can be rewritten as

$$\Delta_A = \tfrac{1}{2}J_0\sin\theta_A/\sin\theta_B , \qquad \Delta_B = \tfrac{1}{2}J_0\sin\theta_B/\sin\theta_A , \tag{4.14}$$

with the restriction that $\sin\theta_A \neq 0$ and $\sin\theta_B \neq 0$.

The lower branch of the excitation spectrum $E^-_{\vec{\lambda}}$ is proportional to $\vec{\lambda}$ for small λ. It is then gapless and corresponds to the Goldstone mode. The existence of this gapless branch is due to the fact that the magnetization vectors can freely rotate in the XY plane. The two branches of the spectrum $E^{\pm}_{\vec{\lambda}}$ are shown in Fig. 5 as the dotted curves for $n = 1.1$ and $K_0/J_0 = 1.1$. From the energies of various phases given in the last section, it is easy to obtain

$$K_0/J_0 = [1+(n-1)^2]/[1-(n-1)^2]$$

to determine the boundary between the M and the SS phases. On this boundary we have $\cos\theta_A = \cos\theta_B = n-1$ and so $\Delta_A = \Delta_B = \frac{1}{2}J_0$. Therefore, the excitation spectrum $E^{\pm}_{\vec{\lambda}}$ becomes doubly degenerate and gapless with the dispersion relation

$$E^2_{\vec{\lambda}} = J_0^2 - J^2_{\vec{\lambda}} . \tag{4.15}$$

The spectrum $E_{\vec{\lambda}}$ is plotted in Fig. 5 as curve Q for $K_0/J_0 = 1.1$ and $n = 1.218$.

For finite temperatures, the general temperature-

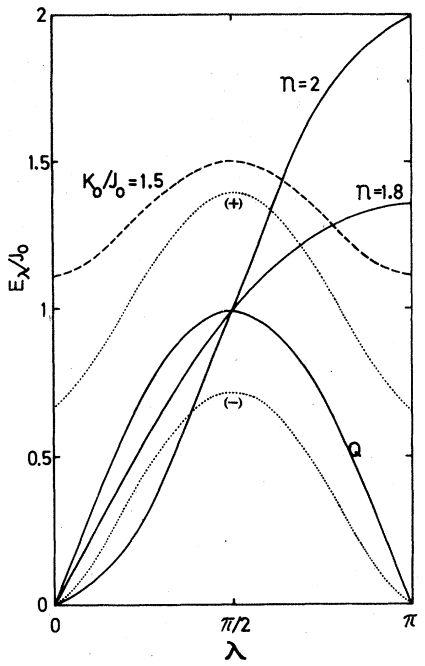

FIG. 5. Dispersion curves for the elementary excitations from various MFA states. See the text for details.

dependent solutions of Eq. (4.10) are obtained as

$$(E_{\vec{\lambda}}^{\pm})^2 = 2(\Delta_A^2+\Delta_B^2) + a_{\vec{\lambda}+}^{A} a_{\vec{\lambda}+}^{B} - a_{\vec{\lambda}-}^{A} a_{\vec{\lambda}-}^{B} \pm \sqrt{\xi_{\vec{\lambda}}} \ , \tag{4.16}$$

where

$$\xi_{\vec{\lambda}} = 4(\Delta_A^2-\Delta_B^2) + 4a_{\vec{\lambda}+}^{A} a_{\vec{\lambda}+}^{B} (\Delta_A+\Delta_B)^2 - 4a_{\vec{\lambda}-}^{A} a_{\vec{\lambda}-}^{B} (\Delta_A-\Delta_B)^2 + (a_{\vec{\lambda}-}^{A} a_{\vec{\lambda}+}^{B} - a_{\vec{\lambda}+}^{A} a_{\vec{\lambda}-}^{B})^2 \ . \tag{4.17}$$

The temperature dependence of the spectrum is due to the temperature dependence of the $D_{\alpha\beta}^{i}$ in Eq. (4.12). With little effort one can check that the lower branch is gapless, in agreement with the gapless branch in the ground state. One can also check that at the SS-M phase boundary the upper branch becomes soft.

B. Charge-ordered phase

Since we have $(\theta_A,\theta_B)=(0,\pi)$ or $(\pi,0)$ for the charge-ordered phase, Eq. (4.10) is simplified to

$$\begin{bmatrix} E-2B-K_0 D_{+-}^{B} & -J_{\vec{\lambda}} D_{+-}^{A} \\ J_{\vec{\lambda}} D_{+-}^{B} & E-2B+K_0 D_{+-}^{A} \end{bmatrix} \begin{bmatrix} G_{+-+}^{AB}(\vec{\lambda},E) \\ G_{+--+}^{BB}(\vec{\lambda},E) \end{bmatrix} = \frac{1}{2\pi} D_{+-}^{B} \begin{bmatrix} 0 \\ 1 \end{bmatrix} \ . \tag{4.18}$$

The excitation spectrum can then be solved as

$$E_{\vec{\lambda}}^{\pm} = 2B - K_0(n-1) \pm \{K_0^2\eta^2 + [(n-1)^2-\eta^2]J_{\vec{\lambda}}^2\}^{1/2} \ . \tag{4.19}$$

The effective field B and the charge-ordering parameter η are determined by the two coupled equations (3.24) and (3.25). At zero temperature and with $n=1$ Eq. (4.19) reduces to the correct form with double degeneracy $E_{\vec{\lambda}}^2 = K_0^2 - J_{\vec{\lambda}}^2$. The spectrum for $K_0/J_0=1.5$ and $n=1$ is shown in Fig. 5 as the dashed curve. For the case of $K_0/J_0=1$ and $n=1$, the spectrum is indistinguishable from the curve Q.

Since $\eta \to 0$ as the boundary between the charge-ordered and the nonordered phases is approached, on this boundary we can see with the help of Eqs. (3.24)–(3.26) that Eq. (4.19) becomes

$$E_{\vec{\lambda}}^{\pm} = n(1-\tfrac{1}{2}n)K_0 \ln\frac{n}{2-n} \pm (n-1)J_{\vec{\lambda}} \ . \tag{4.20}$$

At the multicritical point, from Eqs. (3.26) and (3.29) we derive from the relation $T(\mathrm{CO})=T(\mathrm{SS})$ that

$$n(1-\tfrac{1}{2}n)K_0 \ln\frac{n}{2-n} = (n-1)J_0 \ .$$

Equation (4.20) then turns out to be

$$E_{\vec{\lambda}}^{\pm} = (n-1)(J_0 \pm J_{\vec{\lambda}}) \ . \tag{4.21}$$

Consequently, the gap of the lower branch of the excitation spectrum gradually diminishes as the multicritical point is approached along the charge-ordered and the nonordered phase boundary.

C. Singlet-superconducting phase

Since in this phase $\theta_A=\theta_B$, the indices which label the sublattices can be omitted. The equation of motion (4.8) yields the following two equations

$$\begin{bmatrix} E-J_0 D_{+-}+(J_{\vec{\lambda}}+J_{\vec{\lambda}}\cos^2\theta-K_{\vec{\lambda}}\sin^2\theta)M & -M(J_{\vec{\lambda}}+K_{\vec{\lambda}})\sin^2\theta \\ M(J_{\vec{\lambda}}+K_{\vec{\lambda}})\sin^2\theta & E+J_0 D_{+-}-(J_{\vec{\lambda}}+J_{\vec{\lambda}}\cos^2\theta-K_{\vec{\lambda}}\sin^2\theta)M \end{bmatrix} \begin{bmatrix} G_{+-\beta\beta'}(\vec{\lambda},E) \\ G_{-+\beta\beta'}(\vec{\lambda},E) \end{bmatrix} = \frac{1}{2\pi} D_{+-} \begin{bmatrix} \delta_{+\beta'}\delta_{\beta-} \\ -\delta_{-\beta'}\delta_{\beta+} \end{bmatrix} \ , \tag{4.22}$$

with $(\beta\beta')=(+-)$ or $(-+)$. M is determined by Eq. (3.28) and $\cos\theta=(n-1)/2M$. We can then easily obtain the excitation spectrum as

$$E_{\vec{\lambda}} = 2M[(J_0-J_{\vec{\lambda}}\cos^2\theta+K_{\vec{\lambda}}\sin^2\theta)(J_0-J_{\vec{\lambda}})]^{1/2} \ . \tag{4.23}$$

Therefore, the elementary excitation is a gapless Goldstone mode. For $K_0/J_0=2$ the spectra are shown in Fig. 5 as solid curves for $n=1.8$ and 2.

For $n=n_c=1.577$, the spectrum is indistinguishable from the curve Q. We would like to point out that our conclusion concerning the gapless spectrum agrees with the exact results of the one-dimensional Hubbard model with AII,[23,59] which is a special case of our treatment with $K_0/J_0=1$.

At the temperature $T(\mathrm{SS})$, using the information of $\theta=0$ and Eqs. (3.28) and (3.29), Eq. (4.23) is simplified to

$$E_{\vec{\lambda}} = |n-1|(J_0-J_{\vec{\lambda}}) \ . \tag{4.24}$$

We see then approaching the singlet-superconducting and the nonordered phase boundary, the dispersion relation changes from the quadratic character to the linear character. This is due to the dynamical enhancement of symmetry at the phase boundary.

D. Nonordered phase

In this case the equation of motion (4.8) has the simple solution

$$G_{+--+}(\vec{\lambda},E)=\frac{n-1}{2\pi}(E-E_{\vec{\lambda}})^{-1} , \tag{4.25}$$

where

$$E_{\vec{\lambda}}=\frac{1}{\beta}\ln\frac{n}{2-n}-(n-1)J_{\vec{\lambda}} . \tag{4.26}$$

The spectrum has a gap which vanishes on the singlet-superconducting and the nonordered phase boundary, as well as at the multicritical point.

E. Summary

Since for $K_0/J_0>1$ there are four phases and four phase boundaries meeting at a multicritical point, the elementary excitations from states corresponding to various parts of the phase diagram are somewhat complicated. In Fig. 5 we have shown only a few spectra to illustrate the main features. To close up this section, it is helpful to summarize the general features of these excitation spectra.

Let us use Fig. 4(b) as our reference phase diagram. We will first consider the case of finite temperatures. In the CO phase and on the CO-NO boundary, the excitation spectrum consists of two branches both of which have gaps. Approaching the CO-M phase boundary, the gap of the lower branch decreases continuously and disappears at the CO-M phase boundary. The situation of two branches, one with a gap and the other gapless, persists throughout the M phase. Towards the M-SS phase boundary, the upper branch with a gap gets soft. For the SS phase as well as for the SS-NO boundary, the spectrum has only one branch and is gapless. There is also only one branch in the NO phase, but the spectrum has a gap. At the MP point one branch of the spectrum has a gap while the other is gapless.

For zero temperature, the spectrum in the SS phase is gapless. At the boundary between the SS and the M phases, two gapless branches appear but are degenerate. Going into the M phase one branch remains gapless while the other has a gap. At the boundary between the M and the CO phases, i.e., at $n=1$, the two branches become degenerate again. If $K_0/J_0=1$, the degenerate spectrum is gapless. If $K_0/J_0>1$, the degenerate spectrum has a gap.

V. DISCUSSION

The canonical transformation Eq. (2.5) with $\vec{Q}=0$ has been used by several authors to derive the equivalent Hamiltonian Eq. (2.8) with intra-atomic repulsion from the Hamiltonian Eq. (2.1) with intra-atomic attraction. However, such transformation does not simplify the problem unless $n=1$. We have made use of the absence of magnetic ordering in the Hamiltonian Eq. (2.1), and this property expressed as Eq. (2.3) introduces the additional information Eq. (2.11) that the quasiparticle density $\bar{n}$ is just 1. This we believe is one major contribution to the investigation of the extended Hubbard model with AII.

To derive the antiferromagnetic Heisenberg-type Hamiltonian from the Hubbard Hamiltonian at the strong U limit has also been commonly used by many authors. Our effective pseudospin Hamiltonian Eq. (2.17) is more general including the anistropic term and the effective random external magnetic field. Yet the more important factor, which in our opinion is the second major contribution of the present work, is the constraint Eq. (2.18) on the magnetization. As we have discussed at the end of Sec. III, the new features in our phase diagram as compared to the phase diagram of the ordinary anisotropic antiferromagnet are entirely due to this constraint.

The elementary excitations from the MA states exhibit interesting but rather complex behavior. Although we have derived the analytical for the excitation energy, the dispersion relation will be too complicated to be visualized without numerical examples. Figure 5 is the result of a one-dimensional calculation for simplicity. However, its characteristic features are also preserved for higher dimensionalities.

It is interesting to investigate the thermodynamic properties of (2.1) for regimes of weak and intermediate couplings, as well as for the case of random site energy E_i. This will be reported in the near future.

ACKNOWLEDGMENTS

One of us (R.M.) would like to thank Professor N. J. Parada and Conselho Nacional De Desenvolvimento Científico e Tecnológico for hospitality extended to him at Instituto de Pesquisas Espaciais.

*Permanent address.
[1]W. A. Little, Phys. Rev. 134, A1416 (1964).
[2]P. Pincus, Solid State Commun. 11, 51 (1972); R. A. Bari, Phys. Rev. B 9, 4329 (1974).
[3]P. M. Chaikin, A. F. Garito, and A. J. Heeger, Phys. Rev. B 5, 4966 (1972); J. Chem. Phys. 58, 2336 (1973).
[4]G. Beni, P. Pincus, and J. Kanamori, Phys. Rev. B 10, 1896 (1974).
[5]G. V. Ionova, E. F. Makarov, and S. P. Ionov, Phys. Status Solidi (b) 81, 671 (1977).
[6]A. Luther and I. Peschel, Phys. Rev. B 9, 2911 (1974); A. Luther and V. J. Emery, Phys. Rev. Lett. 33, 589 (1974).
[7]H. Gutfreund and R. A. Klemm, Phys. Rev. B 14, 1073, 1086 (1976).
[8]G. E. Gurgenishvili, A. A. Nersesyon, G. A. Kharadze, and L. A. Chobanyan, Physica (Utrecht) 84B, 243 (1976).
[9]N. Meyhard and J. Solyom, J. Low Temp. Phys. 12, 529, 547 (1973).
[10]H. Fukuyama, T. M. Rice, C. M. Verma, and B. I. Halperin, Phys. Rev. B 10, 3775 (1974).
[11]R. A. Lee, T. M. Rice, and R. A. Klemm, Phys. Rev. B 15, 2984 (1977).
[12]V. Suzumura and H. Fukuyama, J. Low Temp. Phys. 31, 273 (1978).
[13]W. N. Prigodin and J. A. Firsov, Zh. Eksp. Teor. Fiz. 76, 736, 1602 (1979) [Sov. Phys. JETP 49, 369, 813 (1979)].
[14]J. J. Andre, A. Bieber, and F. Gautier, Ann. Phys. (Paris) 1, 145 (1976).
[15]M. Takahashi, Prog. Theor. Phys. 42, 1098 (1969).
[16]H. Shiba, Prog. Theor. Phys. 48, 2171 (1972).
[17]P. Pincus, P. Chaikin, and C. F. Coll III, Solid State Commun. 12, 1265 (1973).
[18]Y. Nagaoka, Prog. Theor. Phys. 52, 1716 (1974).
[19]V. J. Emery, Phys. Rev. B 14, 2989 (1976).
[20]V. J. Emery, in *Chemistry and Physics of One-Dimensional Metals,* edited by H. J. Keller (Plenum, New York, 1977), p. 1.
[21]K. B. Efetov and A. I. Larkin, Zh. Eksp. Teor. Fiz. 69, 764 (1975) [Sov. Phys. JETP 42, 390 (1976)].
[22]S. Robaszkiewicz, Phys. Status Solidi (b) 70, K51 (1975); Acta Phys. Pol. A 55, 453 (1979).
[23]M. Fowler, Phys. Rev. B 17, 2989 (1978).
[24]I. E. Dzyaloshinskii and H. I. Larkin, Sov. Phys. JETP 34, 422 (1972) [Zh. Eksp. Teor. Fiz. 61, 791 (1971)].
[25]J. P. Gallinar, Phys. Status Solidi (b) 88, K143 (1978).
[26]P. W. Anderson, Phys. Rev. Lett. 34, 953 (1975); J. Phys. (Paris) 37, C4-339 (1976).
[27]R. A. Street and N. F. Mott, Phys. Rev. Lett. 35, 1293 (1975).
[28]D. Adler and E. J. Yoffa, Phys. Rev. Lett. 36, 1197 (1976).
[29]B. K. Chakraverty, M. J. Sienko, and J. Bonnerot, Phys. Rev. B 17, 3781 (1978).
[30]V. S. Lubimov, G. V. Ionova, O. M. Pachev, L. A. Manakowa, E. F. Makarov, and S. P. Ionov, Phys. Status Solidi (b) 75, 91 (1976); V. S. Lubimov, L. A. Manakowa, E. F. Makarov, and S. P. Ionov, *ibid.* 76, 505 (1976).
[31]M. R. Robin and P. Day, Adv. Radiochem. 10, 247 (1967); P. Day, in *Chemistry and Physics of One-Dimensional Metals,* edited by H. J. Keller (Plenum, New York, 1977).
[32]S. P. Ionov, G. V. Ionova, V. S. Lubimov, and E. F. Makarov, Phys. Status Solidi (b) 71, 11 (1975).
[33]S. P. Ionov, V. S. Lubimov, G. V. Ionova, G. V. Uimin, and E. F. Makarov, Phys. Status Solidi (b) 72, 515 (1975).
[34]S. Robaszkiewicz, Phys. Status Solidi (b) 59, K63 (1973); Acta Phys. Pol. A 45, 289 (1974).
[35]G. Röpke, B. Albani, and W. Shiller, Phys. Status Solidi (b) 69, 45 (1975).
[36]A. Richter and J. Mizia, Phys. Status Solidi (b) 92, 519 (1979).
[37]K. A. Chao, R. Micnas, and S. Robaszkiewicz, Phys. Rev. B 20, 4741 (1979).
[38]F. Brouers, J. Phys. F 7, L87 (1977).
[39]W. J. Krivnov and A. R. Ovchinnikov, Zh. Eksp. Teor. Fiz. 67, 1568 (1974) [Sov. Phys. JETP 40, 781 (1974)].
[40]E. Lieb and F. Wu, Phys. Rev. Lett. 20, 1445 (1968).
[41]K. Dichtel, R. J. Jelitto, and H. Koppe, Z. Phys. 246, 248 (1971).
[42]J. Mertsching, Phys. Status Solidi (b) 82, 289 (1977).
[43]H. Matsuda and T. Tsuneto, Prog. Theor. Phys. Suppl. 46, 411 (1970).
[44]M. Cyrot, Physica (Utrecht) 91B, 141 (1977); R. DeMarco, E. N. Economou, and D. C. Licciardello, Solid State Commun. 21, 687 (1977); E. N. Economou, C. T. White, and R. DeMarco, Phys. Rev. B 18, 3946 (1978); C. T. White and E. N. Economou, *ibid.* 18, 3959 (1978); R. DeMarco, E. N. Economou, and C. T. White, *ibid.* 18, 3968 (1978).
[45]P. W. Anderson, Phys. Rev. 115, 2 (1959); in *Solid State Physics,* edited by F. Seitz and D. Tunnbull (Academic, New York, 1963), Vol. 14 p. 99.
[46]K. Keffer, *Hanbuch der Physik* (Springer, Berlin, 1966), Vol. XVIII/2, p. 1.
[47]S. V. Vonsovskii, *Magnetism* (Nauka, Moscow, 1971), p. 679 (in Russian).
[48]T. Matsubara and H. Matsuda, Prog. Theor. Phys. 16, 569 (1956); 17, 19 (1957).
[49]K. S. Liu and M. E. Fisher, J. Low Temp. Phys. 10, 655 (1973).
[50]S. V. Tyablikov, *Method in the Quantum Theory of Magnetism* (Plenum, New York, 1967).
[51]A. D. Bruce and A. A. Aharony, Phys. Rev. B 11, 478 (1975).
[52]J. M. Kosterlitz, D. R. Nelson, and M. E. Fisher, Phys. Rev. B 13, 412 (1976).
[53]M. E. Fisher and D. R. Nelson, Phys. Rev. Lett. 32, 1350 (1974).
[54]J. Hubbard, Proc. R. Soc. London Ser. A 285, 542 (1965).
[55]S. B. Halley and P. Erdös, Phys. Rev. B 5, 1106 (1972).
[56]D. N. Zubariev, Sov. Phys. Usp. 3, 320 (1960) [Usp. Fiz. Nauk 71, 71 (1960)].
[57]V. G. Vaks, A. I. Larkin, and S. A. Pikin, Zh. Eksp. Teor. Fiz. 53, 281, 1089 (1967) [Sov. Phys. JETP 26, 188, 647 (1968)].
[58]D. H.-Y. Yang and Y.-L. Wang, Phys. Rev. B 10, 4714 (1974).
[59]M. Fowler and M. W. Puga, Phys. Rev. B 18, 421 (1978).